

Dark Andreev States in Superconductors

Andrey Grankin and Victor Galitski¹

¹*Joint Quantum Institute, Department of Physics,
University of Maryland, College Park, MD 20742, USA*

The conventional Bardeen-Cooper-Schrieffer (BCS) model of superconductivity assumes a frequency-independent order parameter, which allows a relatively simple description of the superconducting state. In particular, its excitation spectrum readily follows from the Bogoliubov-de Gennes (BdG) equations. A more realistic description of a superconductor is the Migdal-Eliashberg theory, where the pairing interaction, the order parameter, and electronic self-energy are strongly frequency dependent. This work combines these ingredients of phonon-mediated superconductivity with the standard BdG approach. Surprisingly, we find qualitatively new features such as the emergence of a shadow superconducting gap in the quasiparticle spectrum at energies close to the Debye energy. We show how these features reveal themselves in standard tunneling experiments. Finally, we also predict the existence of additional high-energy bound states, which we dub “dark Andreev states.”

Bardeen-Cooper-Schrieffer theory of superconductivity [1] and Bogoliubov-de Gennes equations have proven to be relatively simple and reliable tools to describe a variety of conventional superconductors. A key simplifying assumption of this approach is that the superconducting order parameter is energy-independent [2]. While it is clearly not the case in any real superconductor, many features such as the quasiparticle spectrum, thermodynamic and electromagnetic properties [1, 2] appear insensitive to this approximation. It is reasonable, because the omitted energy dependence normally does not affect low-energy physics. In contrast, accurate determination of the transition temperature is sensitive to the details of the phonon dispersion, the dynamical screening of Coulomb interaction, and the structure of the superconducting gap. The latter can be obtained from the Migdal-Eliashberg (ME) equations [3, 4] which are integral equations in both energy and momentum.

This Migdal-Eliashberg theory [5] predicts a non-trivial structure of the superconducting gap as a function of *real* frequency. In particular, it was shown that for superconductivity mediated by the Einstein phonon modes [6, 7], the gap function has sharp resonance-like features. In the weak coupling regime, these features can be well approximated by the Lorentz function centered at the Debye frequency. Another interesting real-frequency behavior of the gap function is discussed in [8] where the authors predict the possibility of formation of frequency-domain vortices in the presence of phonon-induced attraction and Coulomb repulsion.

In this work, we study how a frequency-dependent order parameter affects the quasiparticle spectrum and tunneling properties of a superconductor. We assume that the frequency dependence has a Lorentz shape, which corresponds to optical-phonon-mediated pairing [4]. We solve the corresponding generalized BdG equations and show that an additional gap emerges in the quasiparticle spectrum at higher energies. In the case of an SNS junction, we also find that additional Andreev in-gap high-energy states can form. We use analogy with quantum optics to interpret these high-energy

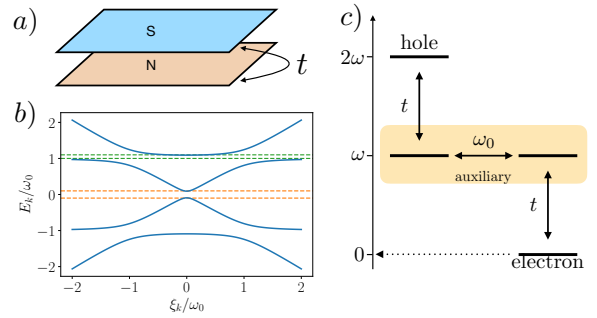


Figure 1. a) Effective proximity system which induces a Lorentz-shape frequency dependence of the order parameter. Fictitious flat-band superconductor shown in blue and a normal-state metal is shown in orange. b) Quasiparticle spectrum of the BdG equation with the frequency-dependent order parameter. Additional band gaps are formed close to the characteristic frequency of the order parameter frequency dependence. Blue solid lines correspond to the eigenenergies of Eq. (3). Orange dashed stands for the conventional BCS gap ($\pm\phi_0$) and dashed green lines $E_k = \omega_0$ and $E_k \approx \omega_0 + \phi_0$ correspond to the additional gap due to the frequency-dependence of the order parameter. In the simulation we assumed $\phi_0 = \omega_0/10$. c) Schematic representation of the four-state system equivalent to the on-shell quasi-electron branch of the BdG Hamiltonian Eq. (4) in the limit of weak coupling $t \rightarrow 0$.

peaks in terms of “dark” resonance features [9–11] of the BdG Hamiltonian with a frequency-dependent order parameter. This suggests a speculation that these finite-energy states could potentially be used to reliably store quantum information.

In this work we consider the conventional s-wave superconductor but keeping a complete realistic frequency dependence of the order parameter. We restrict our discussion to the mean-field level and rely on the Bogoliubov-de Gennes approach, which requires a straightforward generalization. Consider an electron gas with the creation (annihilation) operators $\psi_{\mathbf{k},\sigma=\uparrow,\downarrow}^\dagger$ ($\psi_{\mathbf{k},\sigma}$), where \mathbf{k} denotes the electron momentum. For the two-component spinor $\Psi_{\mathbf{k},n} =$

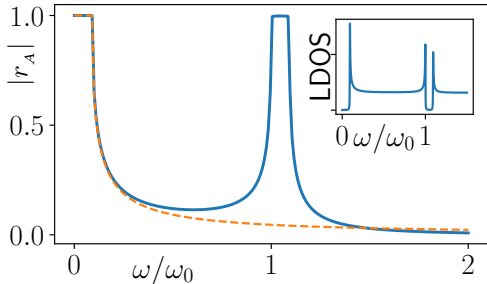


Figure 2. Andreev reflection coefficient as function of the incident electron energy. As result of the additional band gap the additional Andreev reflection peak is observed at energies close to ω_0 . Blue solid line corresponds to the BdG equation with the frequency-dependent anomalous self-energy. Orange dashed stands for the conventional BdG assuming no frequency dependence of the order parameter. Inset shows the local density of states of the Green's function Eq. (1). The gap is chosen such that $\phi_0 = \omega_0/10$.

$\{\psi_{\mathbf{k},\downarrow}(i\varepsilon_n), \psi_{-\mathbf{k},\uparrow}^\dagger(-i\varepsilon_n)\}^T$, the Green function is defined as: $\hat{\mathcal{G}}_{\mathbf{k}}(i\varepsilon_n) \equiv -\langle \Psi_{\mathbf{k},n} \otimes \Psi_{\mathbf{k},n}^\dagger \rangle$, where $\varepsilon_n = (2n+1)\pi/\beta$ is the standard fermionic Matsubara frequency, β is the inverse temperature, and $n \in \mathbb{Z}$. Neglecting the momentum dependence of the self-energy, the Green function of an interacting Fermi gas can be written as [4, 12]:

$$\hat{\mathcal{G}}_{\mathbf{k}}^{-1}(i\varepsilon_n) = i\varepsilon_n \mathcal{Z}_n \hat{\tau}_0 - \phi_n \hat{\tau}_1 - \xi_k \hat{\tau}_3, \quad (1)$$

where $\xi_k = k^2/2m - \mu$, m is the electron mass, μ is the chemical potential, τ_i are Pauli matrices. \mathcal{Z}_n denotes the inverse quasiparticle residue obtained from the odd part of the normal-state self-energy. The off-diagonal matrix element ϕ_n stands for the anomalous self energy. \mathcal{Z}_n and ϕ_n naturally appear in both intrinsic and proximity-induced superconductors [13, 14]. The BdG equations correspond to $\hat{\mathcal{G}}_{\mathbf{k}}^{-1}(i\varepsilon)\chi = 0$, which parameterically determines the sought-after quasiparticle dispersion (here, χ is a Nambu spinor).

To calculate the quasiparticle spectrum, we need an explicit form of the frequency dependence of the anomalous self-energy. In what follows, we consider the aforementioned Lorentz-shaped form (parameterized by its amplitude ϕ_0 and the characteristic frequency ω_0)

$$\phi_n = \phi_0 \frac{\omega_0^2}{\varepsilon_n^2 + \omega_0^2}. \quad (2)$$

As demonstrated in Refs. [6, 7] this solution naturally appears in superconductors, where pairing is induced by an optical phonon mode with the Einstein spectrum at weak coupling. We now consider the spectrum of quasiparticles in Eq. (1).

To develop intuition, it is instructive to consider an auxiliary setup, which involves a fictitious flat-band superconductor with a frequency-independent gap proximity coupled to a normal metal as shown in Fig. 1. As

we show, a proper choice of parameters in this setup gives rise to a Green function, which replicates Eq. 1 with the order parameter (2). The advantage of this construction is that its BdG Hamiltonian below involves only standard, frequency-independent parameters:

$$\hat{\mathcal{G}}_k'^{-1}(i\varepsilon_n) = i\varepsilon_n \hat{\sigma}_0 - \hat{H}_{\text{BdG}} \quad (3)$$

$$H_{\text{BdG}} = \xi_k \hat{\tau}_3 \frac{(\hat{\sigma}_3 + \hat{1})}{2} - \omega_0 \hat{\tau}_1 \frac{(\hat{1} - \hat{\sigma}_3)}{2} + t \hat{\tau}_3 \hat{\sigma}_1, \quad (4)$$

Here $\hat{\tau}_i$ represents Pauli matrices in the Nambu space and $\hat{\sigma}$ parametrizes an effective two-band model: $(\hat{\sigma}_3 + \hat{1})/2$ projects on the normal metal fermion modes and $(\hat{1} - \hat{\sigma}_3)/2$ projector on the fictitious flat-band superconductor. The order parameter in the latter is set the characteristic phonon frequency, ω_0 . We note that we assumed no intrinsic order parameter for the original fermions. The coefficient t denotes the tunneling amplitude between the superconductor and the metal. The auxiliary superconductor can be integrated-out generating both the anomalous and normal self energies. By choosing $t = \sqrt{\phi_0 \omega_0}$ we can exactly match frequency dependence of the order parameter to reproduce Eq. 2. The corresponding \mathcal{Z} -factor in Eq. (1) is equal to $\mathcal{Z}_n = [1 + \phi_0 \omega_0 / (\omega_0^2 + \varepsilon_n^2)] \approx 1$, for $\phi_0 \ll \omega_0$. This procedure effectively replaces the integrating out the bosonic Einstein-phonon degree of freedom (which generates the frequency dependence of the gap in the physical setup) with the integrating out the degrees of freedom of the auxiliary flat-band superconductor. Note that this picture is introduced for the purposes of illustration only. All results can reproduced in the original model directly. As we discuss in the supplementary material, the inverse quasiparticle residue, \mathcal{Z}_n cannot be set identically to one because it would result in an unstable spectrum.

The quasiparticle spectrum can now be found by diagonalizing the static BdG Hamiltonian H_{BdG} given in Eq. (4). The result is shown on Fig. 1 (b) and it has two band gaps. First, we observe the conventional BCS-like band gap at low energies $[-\phi_0, \phi_0]$. It can be obtained by e.g. neglecting the frequency-dependence of the self-energy in Eq. (1), which reduces it to the textbook case. The second band gap at high energies is a specific feature of the two-band system as defined in Eq. (3). As a result of the flatness of one of the dispersion relations, the avoided crossing forms a band gap close to the frequency, ω_0 . The value of this second band gap can be readily obtained analytically from Eq. (3):

$$\phi_2 = \sqrt{\frac{\omega_0}{2} \left(\sqrt{\omega_0(4\phi_0 + \omega_0)} + \phi_0 + \frac{\omega_0}{2} \right)} - \omega_0 \approx \phi_0, \quad (5)$$

where the approximate sign corresponds to the limit $\phi_0 \ll \omega_0$, which must hold for weak coupling.

We now define the local density of states (LDOS) of the electron gas as $\frac{-1}{\pi} \int d\xi_k \text{Im}(G_{\mathbf{k}}(\omega + i0^+))_{1,1}$, where

$G_{\mathbf{k}}$ is the Green function 3 analytically continued to real frequencies. As the direct consequence of the band gap the LDOS is strongly depleted at energies $\approx [\omega_0, \omega_0 + \phi_0]$ as shown on inset in Fig. 2. We note that the exactly zero density of states is a feature of the flat-band dispersion of the auxiliary superconductor/Einstein phonons. However, as we discuss in the SM, introduction of a finite curvature to the phonon dispersion would still lead to a significant depletion of the density of states. As we discuss below this secondary gap can host additional Andreev [15] reflection peaks, observable in metal-superconductor heterostructures.

We now explore how the additional sharp Lorentz-like features of the gap function affect the superconducting proximity effect. In order to describe the transmission and reflection of quasiparticles, we employ the Blonder-Tinkham-Klapwijk (BTK) formalism [16]. We consider a heterostructure consisting of normal and superconducting metals (NS). Following [16], we consider the scattering of an incident electron off of the barrier. The strength of the proximity effect can be characterized by the probability for an electron to scatter into a hole-type excitation.

Within the BTK theory the boundary condition is given by:

$$\vec{\psi}_N(0) = \vec{\psi}_S(0), \quad (6)$$

$$\frac{\partial_z}{2m_N} \vec{\psi}_N(0) = \frac{\partial_z}{2m_S} \vec{\psi}_S(0) + H \vec{\psi}_S(0). \quad (7)$$

where m_S and m_N are the effective electron masses and H is the δ -barrier height. Performing the analytic continuation and replacing $i\epsilon_n \rightarrow \omega + i0^+$, the wavefunctions on superconducting side satisfy the equation $\hat{G}_{\mathbf{k}}^{-1}(\omega + i0^+) \vec{\psi}_S = 0$. On the normal side the equation is the same with the substitution $\phi(\omega + i0^+) \rightarrow 0$ and $\mathcal{Z}(\omega + i0^+) \rightarrow 1$. In the following we do not explicitly write 0^+ for shortness. The normal-state solution representing an incident electron and reflected electron and hole components is:

$$\vec{\psi}_N = \begin{bmatrix} 1 \\ 0 \end{bmatrix} e^{ik_e z} + \begin{bmatrix} r_N \\ 0 \end{bmatrix} e^{-ik_e z} + \begin{bmatrix} 0 \\ r_A \end{bmatrix} e^{ik_h z}, \quad (8)$$

where r_N and r_A denote the reflection amplitude in the electron and hole channels respectively and the electron/hole momenta are given by $k_{e/h} = \sqrt{2m(\mu \pm \omega)}$. Analogously we find the solution for the quasi-electrons and quasi-holes propagating in the superconductor:

$$\vec{\psi}_S \approx C_{qe} \begin{bmatrix} 1 \\ \eta_+ \end{bmatrix} e^{ik_{qe} z} + C_{qh} \begin{bmatrix} 1 \\ \eta_- \end{bmatrix} e^{-ik_{qh} z}, \quad (9)$$

where C_{qe} and C_{qh} are the corresponding amplitudes of the quasi-electron and quasi-holes and we denote the corresponding coherence factors as $\eta_{\pm} =$

$\phi(\omega) / (\mathcal{Z}(\omega)\omega \pm \sqrt{\mathcal{Z}^2(\omega)\omega^2 - \phi^2(\omega)})$. In the quasi-classical limit the quasielectron and quasihole momenta k_{qe}, k_{qh} can be taken to be equal to the corresponding Fermi momenta.

Upon solving the set of equations Eqs. (6-9) in the quasi-classical [17] limit and assuming $m_S = m_N$ we find the Andreev reflection coefficient to be:

$$r_A = \frac{\eta_- \eta_+}{\eta_- + \mathcal{Z}^2(\eta_- - \eta_+)}, \quad (10)$$

$$r_N = \frac{-\mathcal{Z}(i + \mathcal{Z})}{\eta_- + \mathcal{Z}^2(\eta_- - \eta_+)} (\eta_- - \eta_+) \quad (11)$$

where the normalized barrier height is defined as $Z \equiv mH/\sqrt{2m\mu}$. We note that the conventional Andreev reflection can be obtained from Eq. (10) by simply assuming frequency-independent \mathcal{Z} and ϕ . In the limit of $\mathcal{Z} = 0$ the Andreev reflection coefficient is given by $r_A = \eta_+$. We therefore find that in order to have a strong Andreev reflection the condition $\phi \gg \mathcal{Z}\omega$ should be satisfied. The latter condition is always satisfied at very low frequencies leading to the conventional Andreev reflection [15] result $|r_A| \approx 1$. However it can also be satisfied at large frequencies if the frequency-dependent order parameter $\Delta(\omega) \equiv \phi(\omega)/\mathcal{Z}(\omega)$ is larger than the frequency $\Delta(\omega) \gg \omega$. In this case the reflection is up to a possible phase factor identical to the low-energy case. As shown in Fig. 2, this scenario is realized for the Lorentz-like order parameter introduced above in the frequency range close to the resonance $\omega \sim \omega_0$.

Finite-energy bound states – We now consider the possibility of having the finite-energy Andreev bound states [15] in the junction consisting of two superconductors separated by a metallic region with the two boundaries located at $L/2$ and $-L/2$. We assume the phase difference between two superconductors to be γ . In order to find the bound states we now follow the same procedure as for outlined above for the Andreev reflection but matching solutions at the two boundaries simultaneously. The general solution can be obtained analytically but it is too cumbersome and we therefore consider some simple limiting case. In particular as we demonstrate in the supplementary material, in the limit $\phi_0 \ll \omega_0$ and $L \rightarrow 0$ there are two additional in-gap bound states $\omega \in [\omega_0, \omega_0 + \phi_0]$ with the energies ω_{α} (both positive and negative):

$$\omega_{\alpha} = \omega_0 + \frac{1}{2} \left\{ 1 + \alpha \cos \frac{\gamma}{2} \right\}, \quad (12)$$

with $\alpha = \pm$. We thus find the energy of these bound states is of the order of the characteristic frequency of the order parameter frequency dependence. For both intrinsic and proximity superconductors ω_0 can be expected to be of the order of several THz. This implies

the existence of such bound states can potentially be probed by means of laser excitation. Their response is equivalent to a two-level system thus making them a good candidate for realization of solid state qubits.

Interpretation as "dark" resonance – We now discuss the interpretation of the additional Andreev reflection peak in terms of the so-called “dark” resonance. The concept of dark resonance is extensively studied within the field of quantum optics [10]. It is based on the existence of “slowly”-evolving superposition states in a quantum system which are decoupled from the “fast” e.g. environment modes. For example, such optical phenomena as the Electromagnetically Induced Transparency (EIT) [9] are based on the existence of a dark resonance in a driven three-level system. The on-shell BdG Green’s function Eq. (3), can be expressed as follows:

$$\hat{G}'_{\mathbf{k} \rightarrow \mathbf{k}(\omega)}(\omega + i0^+) = \begin{pmatrix} \omega - \xi_{\pm}(\omega) & 0 & t & 0 \\ 0 & \omega + \xi_{\pm}(\omega) & 0 & -t \\ t & 0 & \omega & \omega_0 \\ 0 & -t & \omega_0 & \omega \end{pmatrix}$$

where $\xi_{\pm}(\omega) = \pm \sqrt{((t^2 - \omega^2)^2 - \omega^2 \omega_0^2) / (\omega^2 - \omega_0^2)}$ is the on-shell quasi-electron and quasi-hole dispersions. By construction the Green function has the flat-band superconducting degree of freedom, which can be considered “slow.” By “dark” we thus define states, which have projection onto the auxiliary degrees of freedom only. Let us now find the quasi-electron and quasi-hole coherence vectors corresponding to the on-shell Green’s function Eq. (3, 4). The latter is schematically shown in Fig. 1 (c) in the limit of $t \rightarrow 0$. At frequencies $\omega \approx \omega_0$ one of the eigenstates of the auxiliary degrees of freedom crosses $\omega = 0$ therefore being degenerate with the electron branch. The corresponding eigenvector is readily found to be given by $\approx [0, 0, 1, 1]^T / \sqrt{2}$. Thus this vector only has “slow” non-propagating (flat-band) components and are decoupled from the other degrees of freedom.

Einstein phonon model – Finally we demonstrate that key results and conclusions of the toy model, involving the auxiliary superconductor, hold in the physical setup of interest, where the pairing interaction is induced by the optical phonon mode. More specifically we now consider the gap function induced by the interaction with the optical phonon mode with the propagator $\mathcal{D}_{\mathbf{q}}(i\nu_m) = -2\omega_0 / (\omega_0^2 + \nu_m^2)$, where $\nu_m \equiv 2\pi m / \beta$, $m \in \mathbb{Z}$. As we demonstrate in the Supplementary material, the matrix-valued self-energy $\hat{\Sigma}(i\epsilon_n)$ is found by solving the Dyson’s equation. The latter reduces to two coupled equations for the inverse quasiparticle residue \mathcal{Z}_n and the gap function

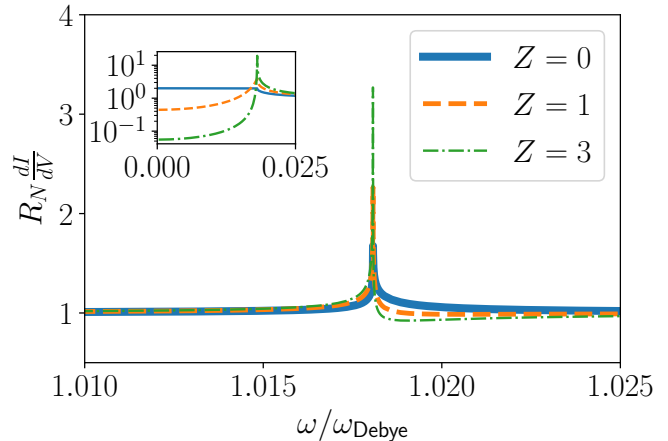


Figure 3. Differential tunneling conductance as function of bias voltage (expressed in frequency units) for different values of the barrier height: $Z = 0$ solid blue, $Z = 1$ dashed orange and $Z = 3$ dot-dashed green. Inset shows the same at low frequencies. The assumed electron-phonon coupling is $\lambda = 0.3$ (see supplementary material). The normal-state resistance is denoted as $R_N = (Z^2 + 1) / (2\nu_0 e^2 \nu_F \mathcal{A})$, where \mathcal{A} is the contact surface area.

ϕ_n in case when the phonon propagator is momentum-independent: $\hat{\Sigma}(i\epsilon_n) = (1 - \mathcal{Z}_n)i\epsilon_n \hat{\tau}_0 + \phi_n \hat{\tau}_1$. The approximate analytical form of the phonon-induced self-energy can be obtained in the limit of weak electron-phonon coupling. As was shown in [6, 7], the imaginary-axis dependence of the order parameter has the Lorentz form $\phi_n \propto \omega_0^2 / (\omega_0^2 + \epsilon_n^2)$ and $\mathcal{Z}_n \approx 1$. This is thus in agreement with the assumed gap-frequency behavior in Eq. (1). At finite electron-phonon coupling strength, the gap frequency dependence deviates from the Lorentz form and additional resonances at frequencies $n\omega_0$ with $n = 1, 2, 3, \dots$ [7] emerge. However, the sharp features of the gap function, reminiscent to the pure Lorentz case, remain even at finite coupling strength [4, 6, 7]. We now study how these features affect the Andreev reflection from the NS boundary. More precisely, we consider the differential tunneling conductance which expresses through the reflection coefficients Eqs. (10, 11) as $dI/dV \propto 1 + |r_A|^2 - |r_N|^2$ [16]. Both reflection coefficients are found numerically by solving the complete set of Migdal-Eliashberg equations. The result of numerical calculation is shown in Fig. 3 for different values of the barrier height Z . We find the prominent additional reflection peaks close to the Debye frequency, which correspond to the dark Andreev resonances. Note that the exact solution for the phonon case involves imaginary self-energy contributions, which give rise to a finite lifetime of the superconducting quasiparticles (absent in the toy model). However, these complications do not appear to affect the qualitative picture and the signatures of the dark Andreev states are preserved.

Conclusions & outlook – In this work, we studied the quasiparticle properties of a superconductor with a frequency-dependent order parameter. When the latter has resonant features, we find an additional depletion of the high-energy density of states. We provide a physically equivalent two-band picture with an additional superconducting band gap emerging at high energies. For the NS junction, the band gap leads to additional Andreev reflection peaks at high energies. In the case of an SNS junction, we find Andreev bound states within the high-energy band gap. We provide an interpretation of these phenomena in terms of the “dark” resonance of the BdG Hamiltonian. We expect that the predicted phenomena should be accessible in experiment in superconductors with optical-phonon-mediated pairing (for example in MgB_2 [18], K_3C_{60} [19], etc) and also proximity systems involving flat-band materials [20]. This work also suggests a number of follow up ideas, at the intersection of superconductivity and quantum optics: e.g., the possibility of control of the dark Andreev states by external laser driving. Furthermore, it would be interesting to explore the role of frequency dependence of the order parameter on the quasiparticle spectrum in topological superconductors and whether dark Majorana-like states are possible.

Acknowledgements – This work was supported by the National Science Foundation under Grant No. DMR-2037158, the U.S. Army Research Office under Contract No. W911NF1310172, and the Simons Foundation. The authors are grateful to Jay Sau for an illuminating discussion.

-
- [1] J. Bardeen, L. N. Cooper, and J. R. Schrieffer, Phys. Rev. **108**, 1175 (1957).
 - [2] A. Altland and B. D. Simons, *Condensed matter field theory* (Cambridge university press, 2010).
 - [3] G. Eliashberg, Sov. Phys. JETP **11**, 696 (1960).
 - [4] F. Marsiglio, Annals of Physics **417**, 168102 (2020), eliashberg theory at 60: Strong-coupling superconductivity and beyond.
 - [5] F. Marsiglio, M. Schossmann, and J. P. Carbotte, Phys. Rev. B **37**, 4965 (1988).
 - [6] F. Marsiglio, Physical Review B **98**, 024523 (2018).
 - [7] S. Mirabi, R. Boyack, and F. Marsiglio, Physical Review B **101**, 064506 (2020).
 - [8] M. H. Christensen and A. V. Chubukov, Physical Review B **104**, L140501 (2021).
 - [9] M. Fleischhauer and M. D. Lukin, Phys. Rev. Lett. **84**, 5094 (2000).
 - [10] M. D. Lukin, S. F. Yelin, M. Fleischhauer, and M. O. Scully, Phys. Rev. A **60**, 3225 (1999).
 - [11] M. Fleischhauer and M. D. Lukin, Physical Review A **65**, 022314 (2002).
 - [12] J. R. Schrieffer, *Theory of superconductivity* (CRC press, 2018).
 - [13] A. V. Chubukov, A. Abanov, I. Esterlis, and S. A. Kivelson, Annals of Physics **417**, 168190 (2020).
 - [14] C.-X. Liu, J. D. Sau, T. D. Stanescu, and S. Das Sarma, Phys. Rev. B **99**, 024510 (2019).
 - [15] J. Sauls, “Andreev bound states and their signatures,” (2018).
 - [16] G. E. Blonder, M. Tinkham, and T. M. Klapwijk, Phys. Rev. B **25**, 4515 (1982).
 - [17] W. Belzig, F. K. Wilhelm, C. Bruder, G. Schön, and A. D. Zaikin, Superlattices and microstructures **25**, 1251 (1999).
 - [18] I. Mazin, O. Andersen, O. Jepsen, O. Dolgov, J. Kortus, A. A. Golubov, A. Kuz’menko, and D. Van Der Marel, Physical review letters **89**, 107002 (2002).
 - [19] F. C. Zhang, M. Ogata, and T. M. Rice, Phys. Rev. Lett. **67**, 3452 (1991).
 - [20] L. Balents, C. R. Dean, D. K. Efetov, and A. F. Young, Nature Physics **16**, 725 (2020).

Supplemental Material for: Dark Andreev States in Superconductors

Andrey Grankin, Victor Galitski

Joint Quantum Institute, Department of Physics, University of Maryland, College Park, MD 20742, USA

I. DERIVATION OF THE GREEN'S FUNCTION IN THE TOY MODEL

In this section we trace-over the auxiliary fermionic degrees of freedom and derive the Green's function of the superconductor. We start with the BdG Hamiltonian:

$$H_{\text{BdG}} = \xi_k \hat{\tau}_3 \frac{(\hat{\sigma}_3 + \hat{1})}{2} - \omega_0 \hat{\tau}_1 \frac{(\hat{1} - \hat{\sigma}_3)}{2} + t \hat{\tau}_3 \hat{\sigma}_1, \quad (13)$$

The quantum-mechanical action corresponding to Eq. (13) reads:

$$S = - \sum_n \tilde{\Psi}_{\mathbf{k}}^\dagger \hat{G}_{\mathbf{k}}'^{-1}(i\epsilon_n) \tilde{\Psi}_{\mathbf{k}}, \quad (14)$$

where $\tilde{\Psi}$ is the extended Bogolyubov spinor and $\hat{G}_{\mathbf{k}}'^{-1}(i\epsilon_n) = i\epsilon_n - H_{\text{BdG}}$. The partitioning function is related to Eq. (14) $Z = \int d... e^{-S}$. We now perform the Gaussian integral over the auxiliary degrees of freedom parametrized by the projector $Q \equiv (\hat{1} - \hat{\sigma}_3)/2$. The projector onto the remaining fermionic degrees of freedom reads $\mathcal{P} = \mathcal{I} - Q$. The Green's function is straightforwardly found to be:

$$\begin{aligned} \hat{G}_{\mathbf{k}}^{-1}(i\epsilon_n) &= i\epsilon_n - \xi_k \hat{\tau}_3 - t^2 \hat{\tau}_3 \frac{1}{i\epsilon_n + \omega_0 \hat{\tau}_1} \hat{\tau}_3 \\ &= i\epsilon_n - \xi_k \hat{\tau}_3 + t^2 \hat{\tau}_3 \frac{i\epsilon_n - \omega_0 \hat{\tau}_1}{\epsilon_n^2 + \omega_0^2} \hat{\tau}_3 \\ &= i\epsilon_n - \xi_k \hat{\tau}_3 + t^2 \frac{i\epsilon_n + \omega_0 \hat{\tau}_1}{\epsilon_n^2 + \omega_0^2} \end{aligned}$$

We thus find the additional normal- and anomalous self-energies $-t^2 i\epsilon_n / (\epsilon_n^2 + \omega_0^2)$, $-t^2 \omega_0 / (\epsilon_n^2 + \omega_0^2)$. Using $t \equiv \sqrt{\phi_0 \omega_0}$ as discussed in the main text we find

$$\mathcal{Z}_n = \left(1 + \frac{\phi_0 \omega_0}{\epsilon_n^2 + \omega_0^2} \right).$$

A. Instability in the absence of \mathcal{Z}_n

Let us now consider a superconductor with the frequency-dependent order parameter and no renormalization of the normal-state self energy:

$$\hat{G}_{\mathbf{k}}^{-1}(i\epsilon_n) = i\epsilon_n \hat{\tau}_0 - \phi_0 \frac{\omega_0^2}{\epsilon_n^2 + \omega_0^2} \hat{\tau}_1 - \xi_k \hat{\tau}_3, \quad (15)$$

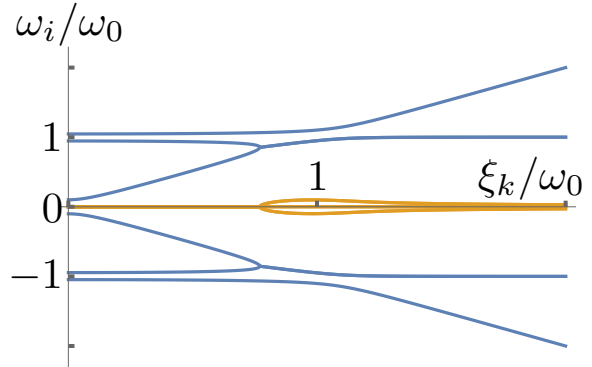


Figure 4. Real (blue) and imaginary (orange) parts of the eigenvalues of the BdG Green's function Eq. (IA). The non-vanishing imaginary parts correspond to the eigenvalues merging close to the ω_0 frequency.

We now find the spectrum of this Greens function and demonstrate that it is unstable.

$$\hat{G}_{\mathbf{k}}^{-1}(\omega + i0^+) = (\omega + i0^+) \hat{\tau}_0 - \phi_0 \frac{\omega_0^2}{\omega_0^2 - (\omega + i0^+)^2} \hat{\tau}_1 - \xi_k \hat{\tau}_3$$

$$\det \hat{G}_{\mathbf{k}}^{-1}(\omega + i0^+) = 0$$

The eigenvalues ω_i are shown in Fig. 4. We find that that the spectrum becomes complex with both positive and negative imaginary values. This corresponds to an unstable system. We thus conclude that the frequency-dependence of the gap implies a presence of a non-zero quasiparticle residue function \mathcal{Z}_n .

II. DERIVATION OF THE GAP FUNCTION AT WEAK COUPLING

Dyson equation for the matrix-valued self energy reads:

$$\hat{\Sigma}_{\mathbf{k}}(i\epsilon_n) = -\frac{g^2}{V\beta} \sum_{\mathbf{q}, m} \mathcal{D}_{\mathbf{k}-\mathbf{k}'}(i\epsilon_n - i\epsilon_{n'}) \left\{ \hat{\tau}_3 \hat{G}_{\mathbf{k}'}(i\epsilon_{n'}) \hat{\tau}_3 \right\} \quad (16)$$

The propagator of the Einstein phonon mode reads

$$\mathcal{D}_{\mathbf{k}-\mathbf{k}'}(i\epsilon_n - i\epsilon_{n'}) = \frac{-2\omega_0}{\omega_0^2 - (i\epsilon_n - i\epsilon_{n'})^2},$$

where ω_0 is the Debye frequency. Taking into account the fact that the phonon propagator does not depend on momentum we can simplify Eq. (16):

$$\hat{\Sigma}(i\varepsilon_n) = -\frac{g^2\nu_0}{\beta} \sum_m \mathcal{D}(i\varepsilon_n - i\varepsilon_{n'}) \int_{-\infty}^{\infty} d\xi_{k'} \left\{ \hat{\tau}_3 \hat{G}_{\mathbf{k}'}(i\varepsilon_{n'}) \hat{\tau}_3 \right\}. \quad (17)$$

The momentum integral $\int d\xi_{k'}$ can be taken analytically by employing the Green's function ansatz Eq. (1).

1. Weak-coupling result

Let us now explicitly find the gap function. Let us first write the complete set of Eliashberg equations as obtained from Eq. (17):

$$Z_n = 1 + \frac{\lambda}{\beta} \sum_m \frac{\omega_0^2}{\omega_0^2 + (\varepsilon_n - \varepsilon_{n'})^2} \frac{\pi \varepsilon_{n'} Z_m}{\sqrt{\varepsilon_{n'}^2 Z_m^2 + \phi_m^2}} \quad (18)$$

$$\Delta_n Z_n = \frac{\lambda}{\beta} \sum_m \frac{\omega_0^2}{\omega_0^2 + (\varepsilon_n - \varepsilon_{n'})^2} \frac{\pi \Delta_m}{\sqrt{\varepsilon_{n'}^2 + \Delta_m^2}}. \quad (19)$$

where we defined $\Delta_m \equiv \phi_m/Z_m$. At very weak coupling we can neglect the non-linearity of both equations or equivalently set $\sqrt{\varepsilon_{n'}^2 + \Delta_m^2} \approx |\varepsilon_{n'}|$. In this case Eq. (19) has logarithmic singularity on the righthand side. Following [6] we can separate singular and regular terms in a straightforward way:

$$\begin{aligned} \Delta_n Z_n &= \frac{\lambda}{\beta} \sum_m \left(\frac{\omega_0^2}{\omega_0^2 + (\varepsilon_n - \varepsilon_{n'})^2} - \frac{\omega_0^2}{\omega_0^2 + (\varepsilon_n)^2} \right) \frac{\pi \Delta_m}{|\varepsilon_{n'}|} \\ &+ \frac{\lambda}{\beta} \sum_m \left(\frac{\omega_0^2}{\omega_0^2 + (\varepsilon_n)^2} \right) \frac{\pi \Delta_m}{|\varepsilon_{n'}|} \end{aligned}$$

The first term to the righthand side is now regular while the second one is singular. It is therefore leading at very weak coupling $\lambda \rightarrow 0$. In this case we get:

$$\Delta_n \propto \frac{\omega_0^2}{\omega_0^2 + (\varepsilon_n)^2}$$

We note that in the limit $\lambda \rightarrow 0$ the anomalous self-energy has the same functional form[6, 7]. Analytical continuation requires some caution and the result will be shown in the section below.

A. Analytic continuation

Following the formulation derived in [5–7] we now perform the so-called iterative analytic continuation procedure of the self-energy Eq. (16). Let us now use the

spectral decomposition of fermionic and bosonic

$$\mathcal{D}(i\varepsilon_n - i\varepsilon_{n'}) = \frac{1}{\pi} \int dx \frac{\text{Im} \{ D^R(x) \}}{x - (i\varepsilon_n - i\varepsilon_{n'})}, \quad (20)$$

$$\hat{G}_{\mathbf{k}}(i\varepsilon_{n'}) = \frac{1}{\pi} \int dy \frac{\text{Im} \{ \hat{G}_{\mathbf{k}}^R(y) \}}{y - i\varepsilon_{n'}}. \quad (21)$$

where D^R and \hat{G}^R stand for the retarded Green's functions. By substituting these expressions into Eq. (16) and taking explicitly the Matsubara-frequency sum over $\varepsilon_{n'}$ we find:

$$\begin{aligned} \hat{\Sigma}(i\varepsilon_n) &= \\ &- g^2\nu_0 \int_{-\infty}^{\infty} \frac{d\xi_k}{\pi^2} \int dx dy \frac{\text{Im} \{ D^R(x) \} \text{Im} \{ \hat{\tau}_3 \hat{G}_{\mathbf{k}}^R(y) \hat{\tau}_3 \}}{y - i\varepsilon_n - x} (n_x + f_y), \end{aligned}$$

where n_x and f_y are respectively bosonic and fermionic occupation numbers. Analytic continuation is readily performed by replacing $i\varepsilon_n \rightarrow \omega + i0^+$.

$$\begin{aligned} \hat{\Sigma}(\omega + i0^+) &= \\ &- g^2\nu_0 \int_{-\infty}^{\infty} \frac{d\xi_k}{\pi^2} \int dx dy \frac{\text{Im} \{ D^R(x) \} \text{Im} \{ \hat{\tau}_3 \hat{G}_{\mathbf{k}}^R(y) \hat{\tau}_3 \}}{y - x - \omega - i0^+} (n_x + f_y) \end{aligned}$$

The integral over y can now be taken explicitly. For that we use the following facts: retarded Green's function only has poles in the lower part of the complex plane.

$$\begin{aligned} \hat{\Sigma}(\omega + i0^+) &= \\ &- g^2\nu_0 \int_{-\infty}^{\infty} \frac{d\xi_k}{\pi} \int dx \text{Im} \{ D^R(x) \} \left\{ \hat{\tau}_3 \hat{G}_{\mathbf{k}}^R(x + \omega) \hat{\tau}_3 \right\} (n_x + f_{x+\omega}) \\ &- \frac{g^2\nu_0}{\beta} \sum_n \int_{-\infty}^{\infty} d\xi_k \mathcal{D}(\omega - i\varepsilon_n) \hat{\tau}_3 \hat{G}_{\mathbf{k}}(i\varepsilon_n) \hat{\tau}_3 \end{aligned}$$

The right-hand side of this expression contains both the Matsubara and the real-frequency Green's function. We can now estimate the gap-frequency function in the limit of very weak coupling. We will be interested in the following quantity (see main text) $\Delta(\omega + i0^+) \equiv \phi(\omega + i0^+)/Z(\omega + i0^+)$.

Let us now derive the real-axis $\lambda \rightarrow 0$ expression for the anomalous self-energy. By taking into account $\text{Im} \{ D^R(x) \} = \pi(\delta(\omega + \omega_0) - \delta(\omega - \omega_0))$ at low we find:

$$\begin{aligned} \hat{\Sigma}(\omega + i0^+) &= \\ &+ g^2\nu_0 \int_{-\infty}^{\infty} d\xi_k \left\{ \hat{\tau}_3 \hat{G}_{\mathbf{k}}^R(\omega_0 + \omega) \hat{\tau}_3 \right\} (n_{\omega_0} + f_{\omega_0+\omega}) \\ &- g^2\nu_0 \int_{-\infty}^{\infty} d\xi_k \left\{ \hat{\tau}_3 \hat{G}_{\mathbf{k}}^R(\omega - \omega_0) \hat{\tau}_3 \right\} (n_{-\omega_0} + f_{-\omega_0+\omega}) \\ &- \frac{g^2\nu_0}{\beta} \sum_n \int_{-\infty}^{\infty} d\xi \mathcal{D}(\omega - i\varepsilon_n) \hat{\tau}_3 \hat{G}_{\mathbf{k}}(i\varepsilon_n) \hat{\tau}_3 \end{aligned}$$

The first term is exponentially suppressed at $T \ll \omega_0$. The second term is non-singular and moreover in the $T \rightarrow 0$ limit it only has contributes at $\omega > \omega_0$. The logarithmically-divergent contribution in the $\lambda \rightarrow 0$ is given by the second term. In this limit the anomalous self-energy obeys:

$$\begin{aligned} \phi(\omega + i0^+) &\approx -\frac{g^2\nu_0}{\beta} \sum_n \int_{-\infty}^{\infty} d\xi_k \mathcal{D}(\omega - i\varepsilon_n) \frac{\phi_n}{\varepsilon_n^2 Z_n^2 + \phi_n^2 + \xi_k^2} - 2\pi i g^2 \nu_0 \theta(\omega - \omega_0) - i g^2 \nu_0 \int d\varepsilon_n \frac{2\omega_0 \text{sign}(\varepsilon_n)}{\omega_0^2 - (\omega - i\varepsilon_n)^2} \\ &= \lambda\pi \int \frac{d\omega_n}{2\pi} \frac{\omega_0^2}{\omega_0^2 - (\omega - i\varepsilon_n)^2} \frac{\phi_n}{\sqrt{\varepsilon_n^2 Z_n^2 + \phi_n^2}} \end{aligned}$$

Under the same assumptions as in Sec. (II 1) we find:

$$\phi(\omega + i0^+) \propto \frac{\omega_0^2}{\omega_0^2 - (\omega + i0^+)^2}.$$

B. Normal state self-energy in the weak-coupling limit

We now consider the diagonal terms of the normal-state self-energy in the limit of weak coupling.

:

$$\vec{\psi}_{S,R} = \begin{bmatrix} 1 \\ \frac{e^{i\gamma} \phi(\omega)}{\mathcal{Z}(\omega)\omega + \sqrt{Z^2(\omega)\omega^2 - \phi^2(\omega)}} \end{bmatrix} C_{\text{qe}}^R e^{ik_{\text{qe}}z} + \begin{bmatrix} 1 \\ \frac{e^{i\gamma} \phi(\omega)}{\mathcal{Z}(\omega)\omega - \sqrt{Z^2(\omega)\omega^2 - \phi^2(\omega)}} \end{bmatrix} C_{\text{qh}}^R e^{-ik_{\text{qh}}z}, \quad (22)$$

$$\vec{\psi}_{S,L} = \begin{bmatrix} 1 \\ \frac{\phi(\omega)}{\mathcal{Z}(\omega)\omega + \sqrt{Z^2(\omega)\omega^2 - \phi^2(\omega)}} \end{bmatrix} C_{\text{qe}}^L e^{-ik_{\text{qe}}z} + \begin{bmatrix} 1 \\ \frac{\phi(\omega)}{\mathcal{Z}(\omega)\omega - \sqrt{Z^2(\omega)\omega^2 - \phi^2(\omega)}} \end{bmatrix} C_{\text{qh}}^L e^{ik_{\text{qh}}z}, \quad (23)$$

$$\vec{\psi}_{\text{N}} = \begin{bmatrix} \alpha_N^+ \\ 0 \end{bmatrix} e^{ik_e z} + \begin{bmatrix} \alpha_N^- \\ 0 \end{bmatrix} e^{-ik_e z} + \begin{bmatrix} 0 \\ \beta^+ \end{bmatrix} e^{-ik_h z} + \begin{bmatrix} 0 \\ \beta^- \end{bmatrix} e^{ik_h z}. \quad (24)$$

In Eq. (22) we introduced an additional global phase factor $e^{i\gamma}$ due to the possible global phase difference between the two superconductors. The problem can be solved numerically or in the limit when the thickness of the normal metal is very thin $L \rightarrow 0$. In this case we just match boundaries between two superconductors:

$$\vec{\psi}_{S,L}(0) \approx \vec{\psi}_{S,R}(0) \quad (25)$$

$$\partial_z \vec{\psi}_{S,L}(0) \approx \partial_z \vec{\psi}_{S,R}(0) \quad (26)$$

These two equations define the spectrum of the bound states. The bound state energy ω_α is readily obtained from the equation:

$$\phi^2(\omega_\alpha) - Z(\omega_\alpha)^2 \omega_\alpha^2 + \phi^2(\omega_\alpha) \cos \gamma = 0$$

1. Real-frequency

$$\Sigma(\omega + i0^+) =$$

$$\begin{aligned} &- 2\pi i g^2 \nu_0 \theta(\omega - \omega_0) - i g^2 \nu_0 \int d\varepsilon_n \frac{2\omega_0 \text{sign}(\varepsilon_n)}{\omega_0^2 - (\omega - i\varepsilon_n)^2} \\ &= -\pi i \lambda \omega_0 \theta(\omega - \omega_0) - \lambda \omega_0 \text{arctanh}\left(\frac{\omega}{\omega_0}\right) \end{aligned}$$

III. HIGH-ENERGY ANDREEV BOUND STATES

We now derive the energy of Andreev bound states appearing at high energy due to the additional band gap. Our consideration is essentially very similar to the derivation of the Andreev reflection coefficient in the main text. In particular we now respectively denote the wave functions of the right and left superconductors as $\vec{\psi}_{S,R}$ and $\vec{\psi}_{S,L}$. Solving the equation of motion in all three media we find

By using the Lorentz-form expressions of ϕ and \mathcal{Z} in the limit $\phi_0 \ll \omega_0$ we find the bound state energies Eq. (9) of the main text.

IV. SPECTRAL FUNCTION

We now study the spectral function of the Green's function. It is defined as:

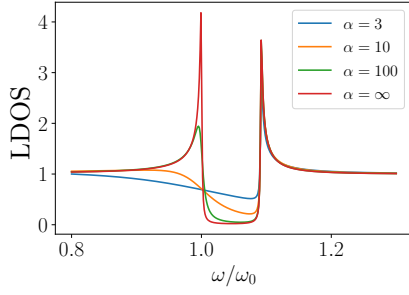


Figure 5. Local density of states in Eq. 27 as function of the mass ratio parameter α .

V. DENSITY OF STATES CALCULATION

In this section we consider the density of states of the superconductor with the BdG Green's function

$$\hat{G}_k^{-1}(\omega + i0^+) = (\omega + i0^+) \mathcal{I}_4 - \begin{pmatrix} \xi_k & 0 & t & 0 \\ 0 & -\xi_k & 0 & -t \\ t & 0 & \xi_k/\alpha & \omega_0 \\ 0 & -t & \omega_0 & -\xi_k/\alpha \end{pmatrix}, \quad (27)$$

This Green's function is almost the same as Eq. 3 in the main text except for instead of the flat-band superconductor we take one with the dispersion ξ_k/α where α denotes the mass ratio parameter. The evolution of density of states as function of α is shown in Fig. 5. We therefore observe a significant density of states depletion for $\alpha \gg 3$.